THIS MONTH IN

JNM

Molecular imaging and RT planning: Grégoire and Chiti provide an overview of current applications and utility of ^{18}F-FDG PET in support of radiation therapy in patients with squamous cell carcinoma of the head and neck. . . . . ***Page 331***

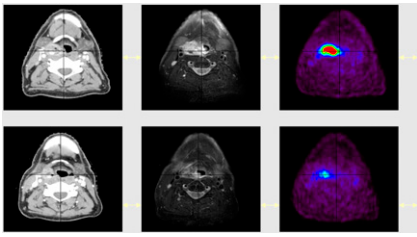

Assessing antiangiogenic response: Beer and Schwaiger review data supporting the use of ^{18}F-fluciclatide PET imaging of $\alpha_v\beta_3$-integrin and $\alpha_v\beta_5$-integrin expression to monitor response to targeted therapy and preview a related article in this issue of *JNM*. . . . . ***Page 335***

Assays of brain efflux transporters: Hall and Pike offer perspective on challenges in development of effective PET radioligands and describe a promising approach that is the focus of a related article in this issue of *JNM*. . . . . ***Page 338***

Staging nasopharyngeal carcinoma: Wu and colleagues report on studies designed to improve detection of intracranial tumor invasion using ^{11}C-choline PET/CT in patients with locally advanced nasopharyngeal carcinoma. . . . . ***Page 341***

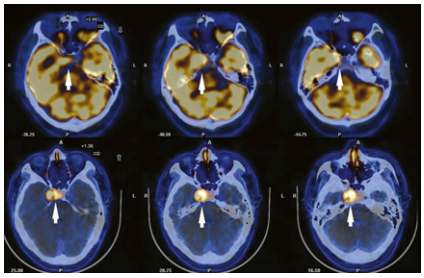

Lesion detection with TOF PET: El Fakhri and colleagues quantify improvements in lung and liver lesion detectability with whole-body time-of-flight PET in oncologic patients with varying body mass indices. . . . . ***Page 347***

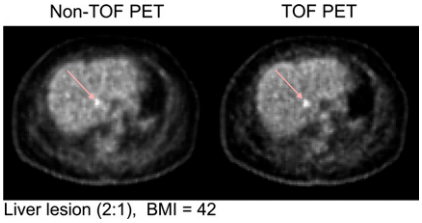

^{18}F-FDG PET/CT and tumor changes: Necib and colleagues propose and evaluate a parametric imaging method for PET/CT assessment of metabolic tumor changes at the voxel level. . . . . ***Page 354***

Carotid ^{18}F-sodium fluoride uptake: Derlin and colleagues correlate ^{18}F-sodium fluoride accumulation in the common carotid arteries of neurologically asymptomatic patients with cardiovascular risk factors and carotid calcified plaque burden. . . . . ***Page 362***

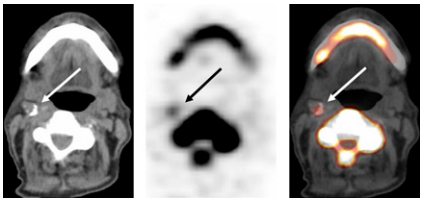

PET textural analysis and response: Tixier and colleagues evaluate new parameters obtained by textural analysis of baseline ^{18}F-FDG PET scans for prediction of therapy response in patients with newly diagnosed esophageal cancer undergoing combined radiochemotherapy. . . . ***Page 369***

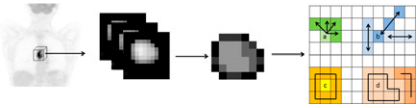

Dynamic PET/CT: Strauss and colleagues describe and investigate shortened acquisition protocols for quantitative assessment of the 2-tissue-compartment model using dynamic ^{18}F-FDG PET/CT. . . . ***Page 379***

Interim PET/CT in large cell lymphoma: Cashen and colleagues look at the effectiveness of ^{18}F-FDG PET/CT in predicting outcomes in patients with advanced-stage diffuse large B-cell lymphoma, with results that raise questions about current interpretation criteria. . . . . ***Page 386***

^{11}C-PIB dual-biomarker imaging: Meyer and colleagues investigate the validity of relative regional cerebral blood flow estimates derived from ^{11}C-labeled Pittsburgh compound B PET as a marker of neuronal activity and neurodegeneration in patients with cognitive impairment. . . . ***Page 393***

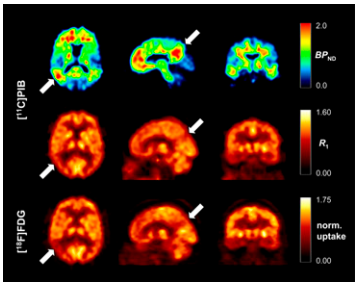

Thalamic nuclei glucose metabolism: Cho and colleagues describe studies measuring substructure-specific metabolic activities in the thalamus with a PET/MRI system made up of ultra-high-resolution PET and ultra-high-field MRI components. . . . . ***Page 401***

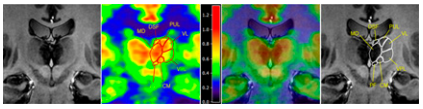

Sentinel node biopsy in breast cancer: Hindié and colleagues provide an educational overview of sentinel node biopsy strategies, with a focus on potential remedies for the relatively high percentage of false-negative results reported. . . . . ***Page 405***

PET radiotracer transport: Tournier and colleagues detail the development of an in vitro model designed to assess the blood–brain barrier transport of selected PET ligands using the concentration equilibrium technique, with potential for screening transport in new drugs. . . . ***Page 415***

^{18}F-fluciclatide PET monitoring: Battle and colleagues use this radiolabeled small peptide, which binds with high affinity to $\alpha_v\beta_3$- and $\alpha_v\beta_5$-integrins, to examine the response of human glioblastoma xenografts to treatment with the antiangiogenic agent sunitinib. . . . . ***Page 424***

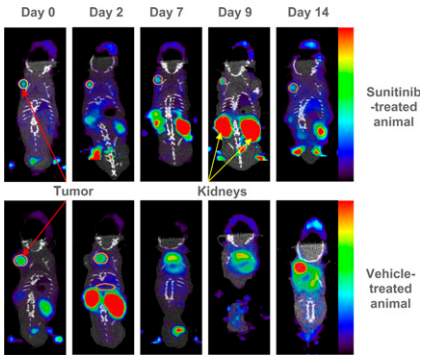

Serial PET lesion evaluation: Heijink and colleagues study information provided by serial ^{18}F-FDG PET imaging in *Apc* mutant mice, which develop multiple intestinal adenomas and are used to study colorectal carcinogenesis and chemopreventive approaches. . . . . ***Page 431***

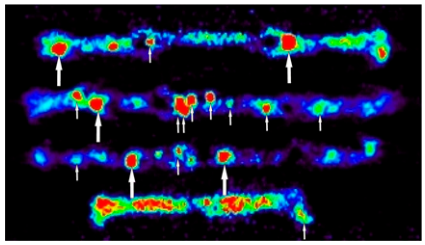

^{18}F-FMISO PET antivascular assessment: Oehler and colleagues explore the utility of ^{18}F-fluromisonidazole PET for monitoring tumor response to a compound that induces rapid endothelial cell apoptosis and decreases perfusion in preexisting tumor vessels.. . . . . ***Page 437***

Imaging intracellular molecular events: Lehmann and colleagues detail the use of avidin–glycosylphosphatidylinositol, an avidin moiety targeted to the extracellular side of cell membranes, as a reporter for in vivo imaging. . . . . ***Page 445***

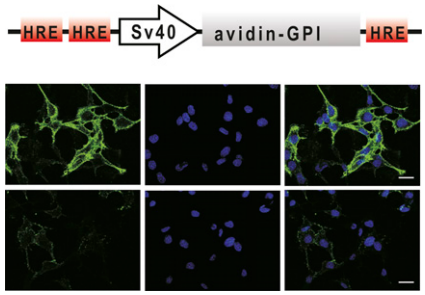

Quantification in myocardial SPECT/CT: Liu and colleagues introduce a heuristic method for correction of extracardiac activity into molecularly targeted SPECT/CT quantification and validate the method for accuracy and reproducibility in a canine model.. . . . . ***Page 453***

^{99m}Tc-labeled recombinant Affibody molecules: Wållberg and colleagues develop an agent with low renal uptake and preserved tumor targeting with promise for development as a diagnostic radiopharmaceutical for imaging of *HER2*-expressing tumors. . . . . ***Page 461***

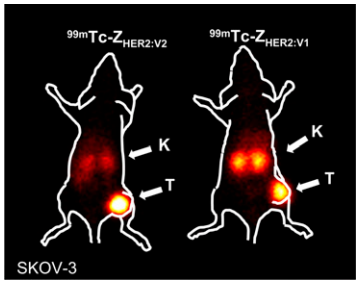

^{64}Cu-SarAr-bombesin imaging: Lears and colleagues describe in vitro and in vivo studies evaluating the internalization of this peptide, which binds with high affinity to the gastrin-releasing peptide receptor, which is overexpressed on a variety of solid tumors. . . . . ***Page 470***

Pharmacokinetics of BBB disruption: Yang and colleagues study the pharmacokinetics of ^{99m}Tc-DTPA in healthy and glioma-bearing rats in the presence of blood–brain barrier disruption induced by focused ultrasound. . . . . ***Page 478***

^{82}Rb stress dosimetry: Senthamizhchelvan and colleagues report on dose estimates under stress for ^{82}Rb, used with PET for cardiac perfusion studies. . . . . ***Page 485***

ON THE COVER

A comparison of digital autoradiography and composite fluorescence images of tumor hypoxia and vasculature. In a study evaluating the ability of ^{18}F-fluoromisonidazole PET to monitor tumor response to an antivascular compound, the pattern of the tracer uptake reflected the effect of the compound on tumor physiology. ^{18}F-fluoromisonidazole distribution was found to be governed by tumor tracer delivery as well as locoregional tumor hypoxia.

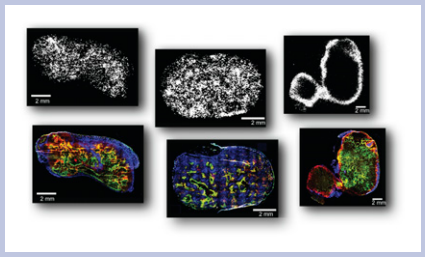

See page 441 and supplemental materials (available online at http://jnm.snmjournals.org).